Investigation of bound state β^- decay half-lives of bare atoms

Shuo Liu, Chao Gao, and Chang Xu [*]
School of Physics, Nanjing University, Nanjing 210093, China

(Received 9 June 2021; accepted 21 July 2021; published 2 August 2021)

We investigate the bound state β^- decay of highly ionized atoms, in which the decay electron remains in a bound atomic state rather than being emitted into the continuum. A survey of 3344 nuclei is performed in order to search possible bound state β^- decay nuclei. We find that, for candidates ^{163}Dy, ^{193}Ir, ^{194}Au, ^{202}Tl, ^{205}Tl, ^{215}At, ^{222}Rn, ^{243}Am, and ^{246}Bk, the channel of β^- decay is completely forbidden in the neutral case but can be opened in the bare case. The corresponding bound-state β^- decay half-lives of these nuclei are predicted by using the Takahashi-Yokoi model, which are found to be significantly different from those in the neutral case.

DOI: 10.1103/PhysRevC.104.024304

I. INTRODUCTION

β^- decay is one of the most important decay modes for unstable nuclei by converting a neutron to proton with an electron and an antineutrino created in continuum states [1]. In 1947, Daudel *et al.* first proposed the concept of bound-state β^- decay and predicted that there might exist nuclear β^- decay accompanied with the electron created directly in an unoccupied atomic orbital [2]. For neutral atoms or moderately ionized atoms, the bound-state β^- decay with electron created in the atomic orbital can hardly proceed. This is because only weakly bound states are available for the decay electron and the bound state β^- decay is only a marginal decay branch. However, for highly ionized atoms, more and more empty states are available and the bound-state β^- transition into deeply bound orbits becomes possible [3]. For instance, with the extremely high temperature and density, the atoms in the stellar plasma are partially or fully ionized and the bound-state β^- decay is found to be important for both the pathways of nucleosynthesis and the abundances of the created nuclide [4,5]. Therefore, the bound-state β^- decay has attracted much attention [6–11] and its first observation was successfully made for ^{163}Dy in 1992 [12]. The question of β^- decay into the bound states was investigated by Batkin in Ref. [13]. Takahashi *et al.* performed a detailed calculation on the β^- decay rates for highly ionized heavy atoms in a plasma of electrons and ions at high temperature and high density [9]. It was found that the bound-state β^- decay channel could lead to a significant change in their total half-lives. For example, the ^{187}Re has an exceptionally long half-life $(4.28 \pm 0.08) \times 10^{10}$ y in the neutral case, which is used to estimate the lower bound for the age of our galaxy [14,15]. However, in the bare case the bound-state β^- decay of ^{187}Re to the first-excited state in ^{187}Os is opened and its total half-life is reduced dramatically from 4.28×10^{10} y to 32.9 y [16].

Previous research into bound-state β^- decay mainly focuses on atoms which are considered to be important for the slow neutron-capture process (*s* process) [10,11]. The *s* process is responsible for the synthesis of approximately half the atomic nuclei heavier than iron via a sequence of neutron captures and β^- decays. For these atoms, the β^- decay process may occur in both the neutral and bare cases. Here we are interested in a special group of atoms, in which the channel of β^- decay is totally forbidden in the neutral case by the energy conservation law, but can be opened in the bare case. To the best of our knowledge, a systematic study on these atoms is still missing. In present work, we perform a survey of 3344 nuclei in the mass range $2 \leqslant A \leqslant 270$ to search for atoms with possible β^- decay channels in the condition of complete ionization. It is found that only a few nuclei satisfy the required energy conditions, namely ^{163}Dy, ^{193}Ir, ^{194}Au, ^{202}Tl, ^{205}Tl, ^{215}At, ^{222}Rn, ^{243}Am and ^{246}Bk. In particular, the bound-state β^- decays of ^{194}Au, ^{202}Tl, ^{215}At, ^{222}Rn, ^{243}Am, and ^{246}Bk have not yet been reported in previous works. Based on the Takahashi-Yokoi model [9], the bound-state β^- decay rates of these nuclei with electrons created in different atomic low-lying states are predicted.

The paper is organized as follows: In Sec. II, we give the energy criteria for selecting bound-state β^- decay nuclei. The formulas of the Takahashi-Yokoi model for calculating the bound-state β^- decay rates are also given. In Sec. III, we discuss the estimated $\log ft$ values and the electron radial wave functions in different atomic low-lying states. The calculated bound-state β^- decay half-lives of suitable candidates are given. Section IV gives a short summary.

II. METHODOLOGY

In the neutral case, the β^- decay energy Q_n is simply the energy corresponding to the mass difference between parent and daughter atoms, and the experimental data of Q_n can be found in Ref. [17]. For the bound-state β^- decay in the bare case, the decay energy Q_b is carried totally by the antineutrino and can be defined as

$$Q_b = Q_n - [B_n(Z+1) - B_n(Z)] + B_{K,L,\ldots}, \tag{1}$$

[*] cxu@nju.edu.cn

TABLE I. The bound-state β^- decay energies of candidate nuclei. Q_n is the β^- decay energy of neutral atoms. $B_n(Z+1) - B_n(Z)$ represents the difference of total electron binding energies between neutral daughter and parent atoms. B_K and B_L are the electron binding energy in atomic K and L shells, respectively. $Q_b(K)$ and $Q_b(L)$ are the bound-state β^- decay energies of fully ionized atoms with electron directly created in atomic K and L shells.

Parent→daughter (g.s.→g.s.)	Q_n (keV)	$B_n(Z+1) - B_n(Z)$ (keV)	B_K (keV)	$Q_b(K)$ (keV)	B_L (keV)	$Q_b(L)$ (keV)
${}^{163}_{66}$Dy → ${}^{163}_{67}$Ho	−2.8	12.5	65.137	49.837	15.746	0.446
${}^{193}_{77}$Ir → ${}^{193}_{78}$Pt	−56.6	15.9	90.660	18.160	22.206	−50.294
${}^{194}_{79}$Au → ${}^{194}_{80}$Hg	−28.0	16.8	95.898	51.098	23.544	−21.256
${}^{202}_{81}$Tl → ${}^{202}_{82}$Pb	−39.2	17.3	101.336	44.836	24.938	−31.562
${}^{205}_{81}$Tl → ${}^{205}_{82}$Pb	−50.7	17.3	101.336	33.336	24.938	−43.062
${}^{215}_{85}$At → ${}^{215}_{86}$Rn	−87.0	18.7	112.844	7.144	27.903	−77.797
${}^{222}_{86}$Rn → ${}^{222}_{87}$Fr	−5.8	19.2	115.859	90.861	28.683	3.685
${}^{243}_{95}$Am → ${}^{243}_{96}$Cm	−7.0	24.0	145.743	114.743	36.493	5.493
${}^{246}_{97}$Bk → ${}^{246}_{98}$Cf	−120.3	23.0	153.124	9.824	38.444	−104.856

where $B_n(Z+1)$ and $B_n(Z)$ are the total electron binding energies of neutral daughter and parent atoms, respectively. $B_{K,L,...}$ is a key quantity for bound-state β^- decay, which represents the binding energy of an electron created in different atomic shells such as K shell or L shell. Because of the contribution of $B_{K,L,...}$, the β^- decay energy Q_b could turn from negative values to positive values. As we are interested in the bound-state β^- decays allowed only in the bare case, the two energy criteria of such decay channels are as follows

$$\text{Energy criterion I, } Q_n < 0$$
$$\text{Energy criterion II, } Q_b > 0. \qquad (2)$$

For the 3344 nuclei throughout the nuclide chart, we found that only a few nuclei ^{163}Dy, ^{193}Ir, ^{194}Au, ^{202}Tl, ^{205}Tl, ^{215}At, ^{222}Rn, ^{243}Am, and ^{246}Bk fulfill the above two energy criterions (see Table I for details). For these nuclei, the β^- decay energies Q_n in the neutral case are all negative and thus the β^- decay channels are completely forbidden. It can also be seen from the difference between $B_n(Z+1)$ and $B_n(Z)$ (for their values, see Ref. [18]) that the absence of the atomic electron ($Z+1 \to Z$) leads to a smaller Q value. However, for bound-state β^- decay with the electron created directly in an unoccupied atomic orbital, Q_b values could become positive due to the additional contribution of B_K or B_L. For all candidates in Table I, the bound-state β^- decay channels with the electron created in the K shell are opened. For ^{163}Dy, ^{222}Rn, and ^{243}Am, the bound-state β^- decays with the electron created in the L shell are also possible.

The bound-state β^- decay rates λ_B of above candidate nuclei are calculated by using the Takahashi-Yokoi model [9–11]:

$$\lambda_B = [\ln 2/(ft)]\, f_m^*, \quad m = a, nu, u, \qquad (3)$$

where $m = a$, nu, and u represents allowed, nonunique first-forbidden and unique first-forbidden transitions, respectively. ft is the comparative half-life which is directly related to the square of nuclear transition matrix element. As mentioned above, the continuum state β^- transitions are energetically forbidden in the neutral case. Therefore, the values of ft cannot be directly obtained, but can be deduced from its inverse process. The method of determining ft values shall be discussed in next section. f_m^* is the lepton phase volume part, described as below [9,19],

$$f_m^* = \sum_x \sigma_x(\pi/2)[f_x \text{ or } g_x]^2 q^2 S_{(m)x}, \qquad (4)$$

where σ_x denotes the vacancy of the electron orbit x, taken as unity in calculations [20]. $[f_x$ or $g_x]$ is the larger component of the electron radial wave functions for the electron orbit x, evaluated at nuclear radius R. $[f_x$ or $g_x]$ is obtained by solving the Dirac bound-state radial equations [21],

$$\frac{dP}{dr} = -\frac{\kappa}{r}P - \frac{E - V(r) + 2m_ec^2}{c\hbar}Q,$$
$$\frac{dQ}{dr} = \frac{E - V}{c\hbar}P + \frac{\kappa}{r}Q, \qquad (5)$$

where E is the energy of electron excluding its rest energy m_ec^2, and the quantum number κ is related to the orbital angular-momentum quantum number l and total angular-momentum quantum number j by [22]

$$\kappa = (l-j)(2j+1) = \left(j + \frac{1}{2}\right)\sigma, \quad \sigma \equiv -\text{sgn}(\kappa) = -\frac{|\kappa|}{\kappa},$$
$$j = |\kappa| - \frac{1}{2} = l + \frac{\sigma}{2},$$
$$l = |\kappa| - \frac{1+\sigma}{2} = j - \frac{\sigma}{2}. \qquad (6)$$

The Dirac bound-state radial wave functions $P(r)$ and $Q(r)$ are normalized to unity,

$$\int_0^\infty [P^2(r) + Q^2(r)]dr = 1. \qquad (7)$$

Here the radial wave functions $P(r)$ and $Q(r)$ are solved by using the subroutine RADIAL [22], which are related to the functions f_x and g_x by

$$f_x = \left(\frac{\bar{\lambda}_c}{a_0}\right)^{\frac{3}{2}} \frac{P(R)}{R}, \quad g_x = \left(\frac{\bar{\lambda}_c}{a_0}\right)^{\frac{3}{2}} \frac{Q(R)}{R}. \qquad (8)$$

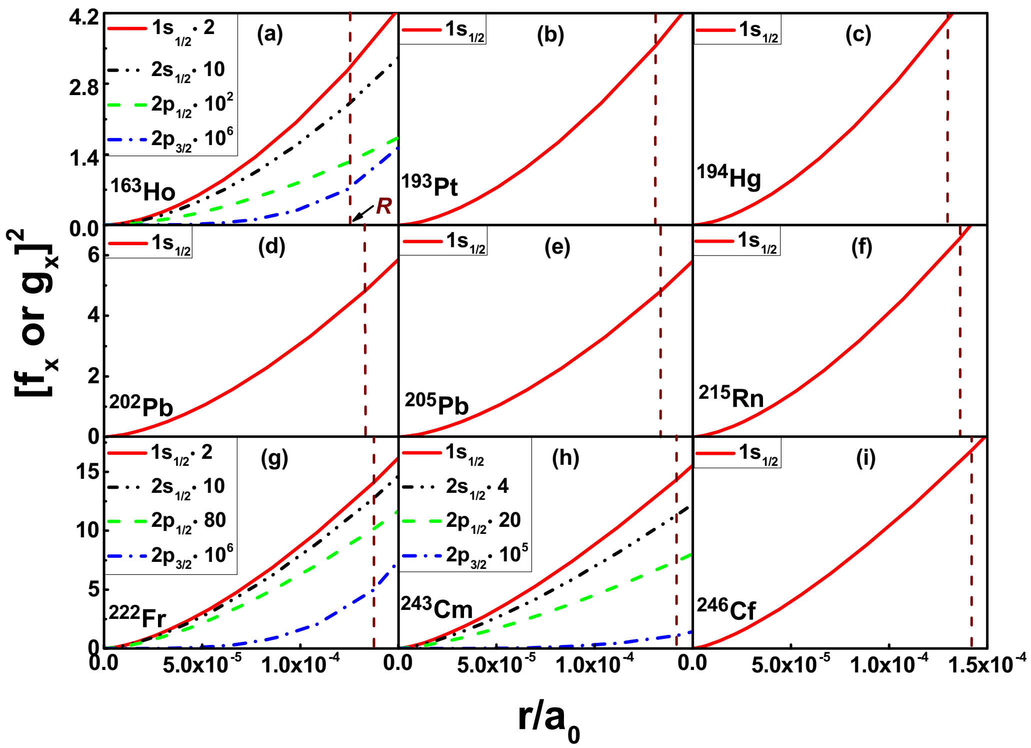

FIG. 1. The squared larger components of the electron radial wave functions for different electron orbitals, in which the magnitude of wave functions is rescaled. The vertical dash line labels the nuclear radius $R = 1.2 \times A^{1/3}$ fm (see the case of ^{163}Ho).

a_0 and $\lambda\!\!\!^{-}_c$ are the Bohr radius and the reduced Compton wavelength, respectively. The nuclear radius is $R = 1.2 \times A^{1/3}$ fm. The finite nuclear size correction of radial wave functions is ignored and its effect is considered to be less than 1% [23]. The detailed discussion of $[f_x$ or $g_x]$ is provided in Sec. III.

The q in Eq. (4) is equal to Q_b/m_ec^2, and $S_{(m)x}$ are the spectral shape factors, given by [9,19]

$$S_{(m)x} = \begin{cases} 1 & \text{for } m = a, nu \text{ and } x = ns_{1/2}, np_{1/2} \\ q^2 & \text{for } m = u \text{ and } x = ns_{1/2}, np_{1/2} \\ 9/R^2 & \text{for } m = u \text{ and } x = np_{3/2}, nd_{3/2} \\ 0 & \text{otherwise.} \end{cases} \quad (9)$$

Note that, although the electron has the possibility to be created in higher atomic shell with large j, however, the influence of this kind of transition is negligible [9].

III. DISCUSSION AND RESULTS

In the Takahashi-Yokoi model, the bound-state β^- decay rate is determined mainly by the nuclear transition matrix element term (i.e., the ft values) and the lepton phase volume term f_m^*. These two important ingredients shall be discussed in detail in this section.

The lepton phase volume f_m^* is related not only to the bound state β^- decay energy Q_b and the spectral shape factor $S_{(m)x}$, but also to the larger components of electron radial wave functions $[f_x$ or $g_x]$. Because the bound-state β^- decay occurs at the place of the transforming nucleon, the electron radial wave functions are approximately evaluated at the nuclear radius R [24]. In Fig. 1, the squared larger components $[f_x$ or $g_x]^2$ (i.e., electron density) of different electron orbitals are shown as a function of r/a_0, where a_0 labels the Bohr radius. The vertical dash line labels the nuclear radius $R = 1.2 \times A^{1/3}$ fm [20]. Note that, for ^{193}Pt, ^{194}Hg, ^{202}Pb, ^{205}Pb, ^{215}Rn, and ^{246}Cf only the wave functions of the K shell ($1s_{1/2}$) are shown because the transitions to the L shell are energetically forbidden. For ^{163}Ho, ^{222}Fr, and ^{243}Cm, the wave functions of both K ($1s_{1/2}$) and L shells ($2s_{1/2}, 2p_{1/2}, 2p_{3/2}$) are shown. Take ^{163}Ho as an example, it is shown that the magnitude of electron density of K shell ($[f_x$ or $g_x]^2$) is much larger than that of L shell at R. For the same L shell, the magnitude of electron density in different states reduces with the increasing of total spin j. Similar behavior can also be found for ^{222}Fr and ^{243}Cm. Therefore, the electrons are much more likely to be created in atomic low-lying states in the process of bound-state β^- decay.

The ft value is the most difficult ingredient in the calculation of bound-state β^- decay rates. As mentioned above, the ft value is closely related to the magnitude of nuclear matrix elements (NMEs) [23]:

$$ft = \frac{2\pi^3 \ln 2}{g^2 |M_{if}|^2}, \quad (10)$$

where g is the weak-interaction coupling constant, and M_{if} is the nuclear transition matrix which consists of both the Fermi and Gamow-Teller terms. Here we estimate the magnitude of NMEs from the time-mirrored orbital electron capture process, i.e., the inverse EC process. As shown in Fig. 2, it

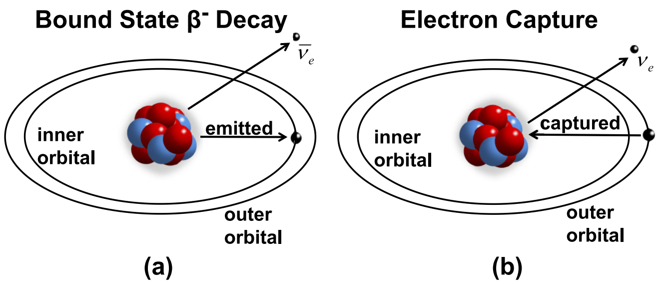

FIG. 2. Schematic view of bound-state β^- decay and inverse orbital electron capture (EC) process. (a) Bound-state β^- decay, in which one neutron in a nucleus decays into proton with monochromatic electron antineutrino emitted and the bound electron created in the inner orbital. (b) Orbital electron capture, in which the bound electron in the outer orbital is captured by the nucleus, transforms a proton into a neutron. The monochromatic electron neutrino is emitted.

is emphasized that the electron accompanied with the bound state β^- decay is bound deeply in the inner orbital, but in the inverse EC process the electron can only be captured from the outer orbital. For instance, the EC decay energies Q_{EC} of ^{163}Ho in the atomic K, L, M, and N shells are

$$\begin{aligned} Q_{EC}(K) &= [M(^{163}\text{Ho})-M(^{163}\text{Dy})]c^2 - B_K = -62.303 \text{ keV}, \\ Q_{EC}(L) &= [M(^{163}\text{Ho})-M(^{163}\text{Dy})]c^2 - B_L = -12.912 \text{ keV}, \\ Q_{EC}(M) &= [M(^{163}\text{Ho})-M(^{163}\text{Dy})]c^2 - B_M = -2.777 \text{ keV}, \\ Q_{EC}(N) &= [M(^{163}\text{Ho})-M(^{163}\text{Dy})]c^2 - B_N = 1.534 \text{ keV}, \end{aligned} \tag{11}$$

where $M(^{163}\text{Ho})$ and $M(^{163}\text{Dy})$ are the masses of parent and daughter atoms, respectively. $B_{K,L,...}$ is the binding energy of an electron captured in different atomic shells. It is seen that the decay energy Q_{EC} is negative for the inner atomic K, L, and M shells, but becomes positive for the outer atomic N shell. The difference between electron binding energies of the inner and outer orbitals is the main reason why the electron can only be captured from the outer orbital in the inverse EC process. Fortunately, the candidates ^{163}Dy, ^{193}Ir, ^{194}Au, ^{202}Tl, ^{205}Tl, and ^{243}Am have well-measured data of the corresponding inverse EC processes. Note that the ratio of transition strengths between the bound-state β^- decay and its inverse EC process depends mainly on the Q value, the spectral shape factor and the electron density, but not on the weak-interaction matrix elements [25]. Therefore, the ft values of the inverse EC process are used as estimated values for the corresponding bound-state β^- decay [see Eq. (3)] [9,12,16]. For the bound-state β^- decays with no inverse EC process, the ft values are estimated from the analogous transitions of neighboring neutral atoms with the same spin and parity [9]. For example, for the transition of $^{193}_{77}\text{Ir}(\frac{3}{2}^+) \to {}^{193}_{78}\text{Pt}^*(\frac{5}{2}^-)$, the $\log ft = 6.46$ is adopted by averaging the $\log ft$ values 6.13, 6.92, and 6.32 of three transitions $^{195}_{77}\text{Ir}(\frac{3}{2}^+) \to {}^{195}_{78}\text{Pt}^*(\frac{5}{2}^-)$, $^{193}_{79}\text{Au}(\frac{3}{2}^+) \to {}^{193}_{78}\text{Pt}^*(\frac{5}{2}^-)$, and $^{195}_{79}\text{Au}(\frac{3}{2}^+) \to {}^{195}_{78}\text{Pt}^*(\frac{5}{2}^-)$ [26,27].

The estimated $\log ft$ values and the bound-state β^- decay half-lives for all candidates are summarized in Table II. The half-lives for their neutral atoms are also given for comparison. The experimental bound-state β^- decay half-life is available only for ^{163}Dy: $T_{\beta_b^-} = 47^{+5}_{-4} d$ [12]. It can be seen from Table II that our calculated half-life $T_{\beta_b^-} = 49.52$ d agrees very well with the data. This is satisfactory because there is no adjustable parameter in our calculations and its

TABLE II. The comparison of bound-state β^- decay half-lives of fully ionized atoms with those of neutral atoms. The second column contains information on the spin and parity of both parent and daughter nuclei and the excitation energies. In the third column, a, nu, or u distinguishes allowed, nonunique first-forbidden or unique first-forbidden transitions, respectively. Q_b is the decay energy for bound-state β^- decay with electron emitted in atomic K shell. The estimated $\log ft$ values are given in column 5. In column 6, we give the experimental half-lives T of all candidates in the neutral case [17], and the predicted bound-state β^- decay half-lives $T_{\beta_b^-}$ are listed in column 7.

Parent→daughter	Transition [E(keV), J^π]	Decay mode	Q_b (keV)	Estimated $\log ft$	Neutral T	Bare $T_{\beta_b^-}$
$^{163}_{66}\text{Dy} \to {}^{163}_{67}\text{Ho}$	$[0.0, \frac{5}{2}^-] \to [0.0, \frac{7}{2}^-]$	a	49.837	4.99	Stable	49.52 d
$^{193}_{77}\text{Ir} \to {}^{193}_{78}\text{Pt}$	$[0.0, \frac{3}{2}^+] \to [0.0, \frac{1}{2}^-]$	nu	18.160	7.16	Stable	65.03 y
$^{193}_{77}\text{Ir} \to {}^{193}_{78}\text{Pt}^*$	$[0.0, \frac{3}{2}^+] \to [1.642, \frac{3}{2}^-]$	nu	16.518	6.63	Stable	23.21 y
$^{193}_{77}\text{Ir} \to {}^{193}_{78}\text{Pt}^*$	$[0.0, \frac{3}{2}^+] \to [14.276, \frac{5}{2}^-]$	nu	3.884	6.46	Stable	282.88 y
$^{194}_{79}\text{Au} \to {}^{194}_{80}\text{Hg}$	$[0.0, 1^-] \to [0.0, 0^+]$	nu	51.098	8.40	38.02 h	122.11 y
$^{202}_{81}\text{Tl} \to {}^{202}_{82}\text{Pb}$	$[0.0, 2^-] \to [0.0, 0^+]$	u	44.836	9.20	12.31 d	1.12×10^5 y
$^{205}_{81}\text{Tl} \to {}^{205}_{82}\text{Pb}$	$[0.0, \frac{1}{2}^+] \to [0.0, \frac{5}{2}^-]$	u	33.336	11.7	Stable	1.16×10^8 y
$^{205}_{81}\text{Tl} \to {}^{205}_{82}\text{Pb}^*$	$[0.0, \frac{1}{2}^+] \to [2.329, \frac{1}{2}^-]$	nu	31.007	5.1	Stable	52.43 d
$^{215}_{85}\text{At} \to {}^{215}_{86}\text{Rn}$	$[0.0, \frac{9}{2}^-] \to [0.0, \frac{9}{2}^+]$	nu	7.144	6.32	0.1 ms	32.95 y
$^{222}_{86}\text{Rn} \to {}^{222}_{87}\text{Fr}$	$[0.0, 0^+] \to [0.0, 2^-]$	u	90.861	8.5	3.82 d	906 y
$^{243}_{95}\text{Am} \to {}^{243}_{96}\text{Cm}$	$[0.0, \frac{5}{2}^-] \to [0.0, \frac{5}{2}^+]$	nu	114.743	7.2	7364 y	0.44 y
$^{243}_{95}\text{Am} \to {}^{243}_{96}\text{Cm}^*$	$[0.0, \frac{5}{2}^-] \to [42.00, \frac{7}{2}^+]$	nu	72.743	6.1	7364 y	31.96 d
$^{246}_{97}\text{Bk} \to {}^{246}_{98}\text{Cf}$	$[0.0, 2^{(-)}] \to [0.0, 0^+]$	u	9.824	9.6	1.80 d	3.49×10^7 y

$\log ft$ value is taken directly from the inverse EC process. For ^{193}Ir, its $\log ft$ value 7.16 of ground-state transition is also taken directly from its inverse process [27]. For the excited-state transition of ^{193}Ir, there is no experimental information on the inverse process and the $\log ft$ value is an averaged one from the neighboring transitions. One may hope to remove the uncertainty of the ft values for bound-state β^- decay by state-of-art calculations of NMEs in future. It is emphasized that the neutral atom of ^{193}Ir is stable, however, its bare atom is predicted to be unstable to β^- decay with a half-life of 16.13 y. Thus the ^{193}Ir could be a good candidate to observe the bound-state β^- decay. The situation of ^{205}Tl is similar to that of ^{193}Ir. The half-life of ^{205}Tl in the bare case is predicted to be 52.43 d and the experiment on ^{205}Tl has already been scheduled at the ESR [28]. For ^{194}Au, ^{202}Tl, ^{215}At, ^{222}Rn, ^{243}Am, and ^{246}Bk, their bound state β^- decay half-lives, to our best knowledge, are predicted for the first time.

Note that the half-lives of neutral ^{194}Au, ^{202}Tl, and ^{246}Bk atoms are determined by the β^+ decay or the EC process [17]. For the neutral ^{215}At, ^{222}Rn, and ^{243}Am atoms, their half-lives are completely determined by the α decay [17]. In the bare case, the bound-state β^- decay channel competes with these decay channels. It can be seen from Table II that the bound-state β^- decay half-lives $T_{\beta_b^-}$ of ^{194}Au, ^{202}Tl, ^{215}At, ^{222}Rn, and ^{246}Bk are much longer than the half-lives of their neutral atoms, showing the bound-state β^- decay is only a marginal decay channel. The neutral ^{243}Am atom has a very long half-life of 7364 y determined totally by the α-decay mode, which is almost not changed in the bare case (less than 1%) [29]. Owing to the bound-state β^- decay, the half-life of bare ^{243}Am atom is predicted to be shortened significantly from 7364 y to 26.66 d, which is also a promising candidate for future bound-state β^- decay experiment.

IV. SUMMARY

To conclude, we found that, for a very small proportion of nuclei throughout the whole chart of nuclides, the channel of bound-state β^- decay is completely forbidden in their neutral atoms but becomes possible in the bare atoms. The corresponding bound-state β^- decay rates are predicted with the $\log ft$ values estimated from the inverse EC process or analogous transitions of neighboring atoms. The half-lives of several candidates are found to be significantly modified as compared with those in the neutral case. In particular, the bound-state β^- decay rates of ^{194}Au, ^{202}Tl, ^{215}At, ^{222}Rn, ^{243}Am, and ^{246}Bk are predicted for the first time. It is suggested that the stable atoms of ^{193}Ir and ^{205}Tl could be suitable candidates for experiments. The half-life of ^{243}Am is found to be shortened significantly from 7346 y to 26.66 d in the bare case, which is also recommended as a hopeful candidate.

ACKNOWLEDGMENTS

The work is supported by the National Natural Science Foundation of China (Grant No. 11822503) and by the Fundamental Research Funds for the Central Universities (Nanjing University).

[1] E. J. Konopinski, Rev. Mod. Phys. **15**, 209 (1943).
[2] R. Daudel, M. Jean, and M. Lecoin, J. Phys. Radium **8**, 238 (1947).
[3] T. Ohtsubo *et al.*, Phys. Rev. Lett. **95**, 052501 (2005).
[4] T. Kodama and K. Takahashi, Nucl. Phys. A **239**, 489 (1975).
[5] L. Senbetu, Phys. Rev. C **7**, 1254 (1973).
[6] S. G. Cohen, Phys. Rev. **84**, 591 (1951).
[7] P. M. Sherk, Phys. Rev. **75**, 789 (1949).
[8] J. N. Bahcall, Phys. Rev. **124**, 495 (1961).
[9] K. Takahashi and K. Yokoi, Nucl. Phys. A **404**, 578 (1983).
[10] K. Takahashi, R. N. Boyd, G. J. Mathews, and K. Yokoi, Phys. Rev. C **36**, 1522 (1987).
[11] K. Takahashi and K. Yokoi, At. Data Nucl. Data Tables **36**, 375 (1987).
[12] M. Jung *et al.*, Phys. Rev. Lett. **69**, 2164 (1992).
[13] I. S. Batkin, Izv. Akad. Nauk SSSR, Ser. Fiz. **40**, 1279 (1976) [Bull. Acad. Sci. USSR, Phys. Sci. **40**, 149 (1976)].
[14] J. M. Luck, J. L. Birck, and C. J. Allegre, Nature (London) **283**, 256 (1980).
[15] D. D. Clayton, Nature (London) **224**, 56 (1969).
[16] F. Bosch *et al.*, Phys. Rev. Lett. **77**, 5190 (1996).
[17] National nuclear data center, https://www.nndc.bnl.gov/.
[18] Atomic Spectra Database, https://physics.nist.gov/PhysRefData/ASD/ionEnergy.html.
[19] Z. Chen, L. Rosenberg, and L. Spruch, Phys. Rev. A **35**, 1981 (1987).
[20] A. Gupta, C. Lahiri, and S. Sarkar, Phys. Rev. C **100**, 064313 (2019).
[21] F. Salvat and J. M. Fernández-Varea, Comput. Phys. Commun. **240**, 165 (2019).
[22] F. Salvat, J. Fernández-Varea, and W. Williamson Jr., Comput. Phys. Commun. **90**, 151 (1995).
[23] N. Gove and M. Martin, At. Data Nucl. Data Tables **10**, 205 (1971).
[24] E. Konopinski and G. Uhlenbeck, Phys. Rev. **60**, 308 (1941).
[25] Y. A. Litvinov and F. Bosch, Rep. Prog. Phys. **74**, 016301 (2011).
[26] X. Huang and M. Kang, Nucl. Data Sheets **121**, 395 (2014).
[27] E. Achterberg, O. Capurro, G. Marti, V. Vanin, and R. Castro, Nucl. Data Sheets **107**, 1 (2006).
[28] M. Steck and Y. A. Litvinov, Prog. Part. Nucl. Phys. **115**, 103811 (2020).
[29] A. Y. Dzyublik, Phys. Rev. C **90**, 054619 (2014).